Peptides 36 (2012) 86–93

Peptides

journal homepage: www.elsevier.com/locate/peptides

The properties conferred upon triple-helical collagen-mimetic peptides by the presence of cysteine residues

David A. Slatter[a,*], Dominique G. Bihan[a], Gavin E. Jarvis[a], Rachael Stone[a], Nicholas Pugh[a], Sumana Giddu[b], Richard W. Farndale[a]

[a] University of Cambridge, Department of Biochemistry, Downing Site, Cambridge CB2 1QW, UK
[b] University of Medicine and Dentistry of New Jersey, Department of Biochemistry, Piscataway, NJ 08854, United States

ARTICLE INFO

Article history:
Received 21 September 2011
Received in revised form 15 April 2012
Accepted 16 April 2012
Available online 23 April 2012

Keywords:
Collagen
Helix
Fiber
Cysteine
Polymer
Oxidation
Cross-link
Adhesion

ABSTRACT

Recently, the ability of polymeric collagen-like peptides to regulate cell behavior has generated great interest. A triple-helical peptide known as collagen-related peptide (CRP) contains the sequence (Gly-Pro-Hyp)$_{10}$. With Gly-Pro-Cys triplets appended to both of its termini, designated CRP$_{cys}$, chemical cross-linking using heterobifunctional reagents generates CRP$_{cys}$-XL, a potent, widely used, polymeric agonist for platelet Glycoprotein VI, whereas non-cross-linked, monomeric CRP$_{cys}$ antagonizes Glycoprotein VI. Here, we describe how cysteine in these triplets may also undergo random air-induced oxidation, especially upon prolonged storage or repeated freeze–thawing, to form disulphide bonds, resulting in a lesser degree of polymerization than with chemical cross-linking. We investigated the monomeric and polymeric states of these and other cysteine-containing collagen-derived peptides, using gel filtration and dynamic light scattering, allowing the size of a CRP-XL aggregate to be estimated. The effect of cysteine thiols upon peptide adsorption to surfaces and subsequent platelet responses was investigated. This demonstrated that cysteine is required for strong binding to glass coverslips and to plastic plates used in ELISA assays.

1. Introduction

Collagens are characterized by the triple-helical structure resulting from the presence of repeating GXX' triplets, where G is glycine, X is commonly proline (P), and X′ is commonly hydroxyproline (O). The fibrillar collagens I and II, whose main triple-helical domains comprise 338 such triplets, are the fundamental scaffolds of the extracellular matrix in bone, tendon (type I), and cartilage (type II) [4,7]. In blood vessel walls and skin, collagen I is interlaced with collagen III, having a 343-triplet helix, whereas non-fibrillar collagen IV networks form basal laminae in structures such as kidney glomeruli, lung alveoli, and blood vessel walls [19]. These collagens, along with the 24 other known collagen types, are widely distributed. Accordingly, a large repertoire of proteins bind to the collagens, including structural components of the extracellular matrix as well as cell receptors that mediate physiological processes such as cell migration, hemostasis, and wound healing.

In 1995, Barnes developed a platelet-reactive model peptide, a GPO polymer now called collagen-related peptide (CRP) [18] which proved to bind the immune receptors, platelet Glycoprotein VI (GpVI) [10,29] and leukocyte-associated immunoglobulin-like receptor-1 (LAIR-1) [14]. Its variant, CRP$_{cys}$ (Table 1) may be chemically cross-linked between its N-terminal amines and cysteine thiols to form soluble aggregates (CRP$_{cys}$-XL) using 3-(2-pyridyldithio)propionic acid N-hydroxy-succinimide ester (SPDP). When CRP$_{cys}$-XL binds GpVI, platelets are activated, leading to their aggregation [11,18].

Subsequently, a small set of triple-helical peptides containing primary sequence from collagen I was used to identify GFOGER as a motif that binds integrins $\alpha1\beta1$ and $\alpha2\beta1$ [12]. To cater for the possibility that cross-linking may similarly be required to support cellular activation via clustering of integrins, these and subsequent peptides, such as GFOGER$_{cys}$ (Table 1), generally included terminal Cys residues. We then synthesized two large sets of peptides (Toolkits) encompassing the entire triple-helical domains of the homotrimeric collagens II and III in 56 and 57 peptides, respectively [3,14]. We use three examples of Toolkit peptides in this paper (Table 1). With the aid of their helix-inducing host sequence, all these peptides fold to form canonical collagen triple helices of similar stability to native collagen [23]. Toolkit peptides have facilitated the systematic mapping of receptors [3,14,33] and structural binding proteins [3,15,16] onto collagens II and III.

* Corresponding author. Current address: University of Cardiff School of Medicine, Tenovus Building, Heath Park, Cardiff CF14 4XN, UK. Tel.: +44 2920 687315; fax: +44 29 2074 3199.
E-mail address: SlatterDA@cardiff.ac.uk (D.A. Slatter).

0196-9781/
http://dx.doi.org/10.1016/j.peptides.2012.04.013

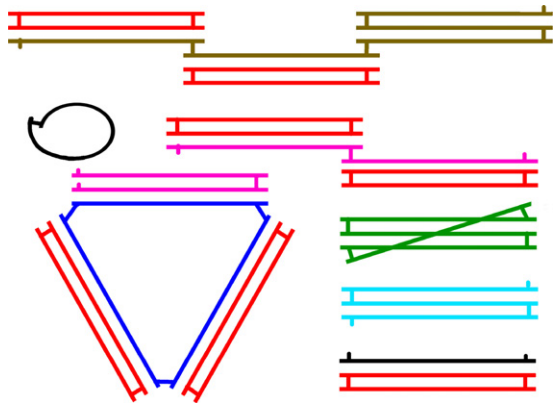

Fig. 1. Peptide complexes that result from cysteine oxidation. Reduced peptide monomers (black line) may become cyclic (black circle), or cross-link with other peptides to form open (pink) and cyclic (red) dimers, open (light blue) and cyclic (dark blue) trimers, or even larger open (brown) and cyclic (green) peptide multimers. Many of these forms can then combine to form triple helices with other peptide monomers or complexes. These complexes may involve parallel triple helices stacked against each other, not shown here for clarity.

Applications for triple-helical peptides may be developed in several ways: the Toolkit approach might be applied to collagen I using heterotrimeric peptides [5,25,28]. Collagen-mimetic peptides are used in biomaterials [24] and may also have diagnostic applications. For example, the identification of a site that bound von Willebrand factor (VWF) using the Toolkits [16] enabled the development of a defined, collagen-mimetic peptide mixture of VWF-, GpVI- and integrin-binding peptides that can support thrombus formation under shear conditions [22], valuable for diagnostic purposes. Although the heterogeneity of these peptides is increased by random oxidation of their terminal cysteine residues (Fig. 1), the latter provide a valuable means of introducing higher-order structure through chemical crosslinking. Their role has not been investigated in any depth, and forms an important focus of this report.

Here, we provide a framework for investigating cross-linked polymeric collagen peptides that complements work on fibril-forming collagen peptides where cysteine aids helix stabilization [13,21]. We also investigate the enhancement of adhesive properties conferred by the oxidation of cysteine upon storage, where the main use of peptides is to investigate cell–collagen interaction using solid-phase adhesion methodology.

Table 1
Peptides used in this study.

Peptide	Sequence (-amide blocked)	Mass (Da)	T_{max}
GFOGER	$(GPP)_9$GFOGER$(GPP)_9$G	5257	nd
$GFOGER_{cys}$	GPC$(GPP)_5$GFOGER$(GPP)_5$GPC	3704	45
B-GFOGER	B-G-3Abu-G$(GPP)_5$GFOGER$(GPP)_5$G	3672	nd
B-$GFOGER_{cys}$	B-GPC$(GPP)_5$GFOGER$(GPP)_5$GPC	3930	nd
CRP	$(GPO)_{10}$G	2747	69
CRP_{cys}	GCO$(GPO)_{10}$GCOG	3294	72
B-CRP	B-G-4Abu-G$(GPO)_{10}$G	3172	nd
GPP_{cys}	GPC$(GPP)_{10}$GPCG	3100	48
B-GPP	B-G-3Abu-G$(GPP)_{10}$G	3012	44
II-56	§-GPRGRSGETGPAGPOGNOGPOGPOGPO-§	5521	59
III-04	§-GPSGPAGKDGESGROGROGERGLOGPO-§	5634	53
III-24	§-GPKGNDGAOGKNGERGGOGGOGPQGPO-§	5500	51

Abu, aminobutyric acid; B, biotin; §, the last three are Toolkit peptides flanked by the host sequences: GPC$(GPP)_5$ (N-terminus) and $(GPP)_5$GPC (C-terminus); T_{max}, helix-unfolding temperature (°C); nd, not done.

2. Materials and methods

2.1. Peptide synthesis

Peptides were synthesized as C-terminal amides on TentaGel R-Ram resin using an Applied Biosystems Pioneer peptide synthesizer as described previously [23]. Fractions containing homogeneous product were identified by analytical HPLC on an ACEphenyl300 (5 μm) column, characterized by MALDI and electrospray mass spectrometry, pooled and freeze-dried. Where applicable, biotin was coupled to the N-terminal group by addition of N-(biotinyloxy)succinimide (5 equiv.) to the peptide resin prior to cleavage. Biotinylation of peptides was found to be effectively 100%. Peptides, listed in Table 1, were checked for helicity [23].

2.2. Peptide oxidation during storage

Samples of Toolkit peptide III-24 and CRP_{cys} were dissolved at 2.5 mg mL^{-1} in cold 10 mM acetic acid. Peptides were held at 4 °C for 2 h, 1 d, 3 d, 14 d, or frozen (−20 °C) for 2 h, 1 d, 3 d, 14 d, or 80 d before immediate gel filtration analysis; a final sample was frozen for 14 d but thawed ten times during that period, mimicking sequential sampling. The experiment was repeated, except that nitrogen was bubbled through the acetic acid for 2 min before using it to dissolve peptide. As peptides are normally stored at 4 °C, we also retrieved 9–48-month-old stock samples of CRP_{cys}, GPP_{cys}, $GFOGER_{cys}$, II-56, III-04 and III-24, all kept at 1 mg mL^{-1} in 10 mM acetic acid. Samples were analyzed using mass-spectrometry, gel filtration, and reduced cysteine quantified using Ellman's reagent, 5,5′-dithio-bis(2-nitrobenzoic acid) (Sigma D8130) [2].

2.3. Synthesis of CRP_{cys}-XL

The heterobifunctional reagent SPDP (Sigma P3415) was dissolved in dry ethanol (50 mM), added to 3 mM peptide predissolved in 0.1 M $NaHCO_3$ (1.5 equiv.), and the mixture flushed with N_2 gas. After 1 h, peptide was dialyzed overnight at 4 °C in 0.01 M acetic acid (one change), stored at 4 °C or freeze-dried and stored at −80 °C.

2.4. Dynamic light scattering (DLS)

Peptide III-24 (2.5 mg mL^{-1}) was dissolved in 10 mM phosphate-buffered saline pH 7.4 containing 2 mM TCEP, heated briefly to 70 °C and allowed to fold for 18 h overnight at 4 °C. It was filtered and loaded into a DynaPro Titan DLS instrument pre-equilibrated at 4 °C. The sample was probed at 4–50 °C, being equilibrated at each temperature for 5 min. Data was handled as previously described [17] and the hydrodynamic radius in nm used to calculate a predicted molecular weight as appropriate for different polymers: a rod-like triple helix, an aggregate of triple helices, or a denatured single chain. We did not observe any collagenous gel formation.

2.5. Gel filtration of peptide

Peptide cross-linking and helicity was measured by preparing 800 μL samples at 0.25 mg mL^{-1} in 10 mM phosphate buffered saline (pH 7.4) and loading onto a Bio-sep Sec-S2000 Gel filtration column (300 mm × 21.2 mm, 5 μM bead size, 14.5 nm average pore size) at 10 °C, equilibrated in the same buffer. Running isocratically, the eluant was monitored at 214 nm. For peptide III-24, the column was additionally run at 40 °C to investigate the increased stability conferred by cross-linking, and peptide III-24, III-04, GPP_{cys}, and $GFOGER_{cys}$, were additionally sampled at 60 °C to obtain a peptide polymer profile (Suppl. Table S1b).

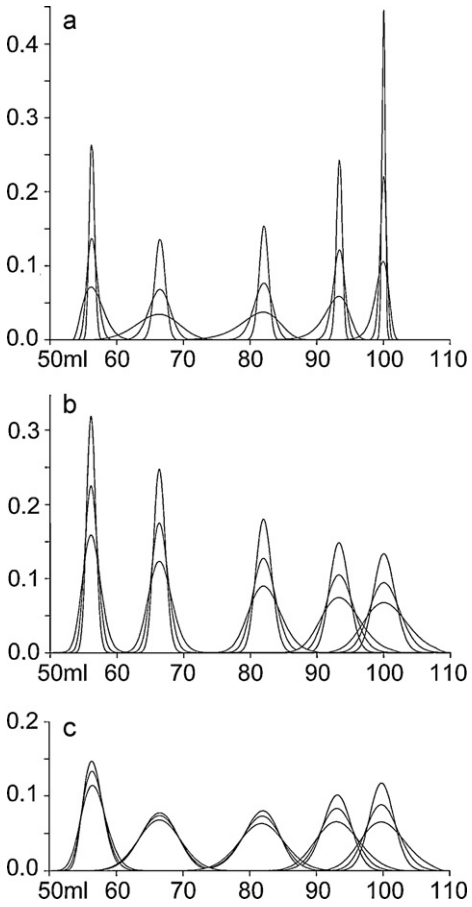

Fig. 2. Modeled gel filtration peaks. Eluted peaks from molecules of Stokes Radius 7, 4, 2, 1, and 0.5 nm are modeled for a Bio-sep Sec-S2000 column (average pore size = 14.5 nm), larger molecules eluting first. (a) Effect of variable pore sizes within the column beads of 14.5 ± 0.5 nm (sharp peaks), 14.5 ± 1 nm, and 14.5 ±2 nm (broad peaks), with no peak broadening due to axial dispersion. (b) Effect of an axial dispersion coefficient (L) of 0.5 $cm^2\ h^{-1}$ (sharp peaks), 1 $cm^2\ h^{-1}$, and 2 $cm^2\ h^{-1}$ (broad peaks) with no peak broadening due to variable pore sizes. (c) Combining both effects, we show elution from a virtual column with pore sizes of 14.5 ± 1.5 nm with an axial dispersion coefficient of 0.5 $cm^2\ h^{-1}$ (sharp peaks), 1 $cm^2\ h^{-1}$ (average), and 2 $cm^2\ h^{-1}$ (broad peaks).

Overlapping gel filtration sample peaks derived from different peptide polymers require mathematical deconvolution into components. Three major effects describe a gel filtration peak: first, bead pore size and homogeneity ($r \pm \sigma$, Fig. 2a, Suppl. Section 2.10); second, diffusion and inhomogeneity of flow, using the axial dispersion coefficient, L (Fig. 2b and Suppl. Section 2.11); third, solute interactions. To reduce the dimensionality of the model, we allowed an increase in L to include solute interactions (Suppl. Section 2.12). We combined these effects by allowing σ and L to vary, modeled in Fig. 2c, and fitted multiple peaks to each dataset (Suppl. Section 2.13).

Overlapping peaks in our results could represent TCEP; non-helical peptide; N- to C-terminal cyclic cross-linked non-helical peptide monomer; cross-linked non-helical peptide dimers; cross-linked cyclic dimeric peptide; peptide triple helix; cross-linked triple helix dimers; small groups of (∼3–5) cross-linked triple helices; and larger groups of (6+) cross-linked triple helices. The last four classes are heterogeneous and could not be fully resolved, so it was decided to fit a peak representing a variety of molecule sizes, for instance, grouping all 3–5 helix aggregates under one fitted peak. The deconvolution was used to present data giving the percentages of peptide in each peptide form (Figs. 3–5).

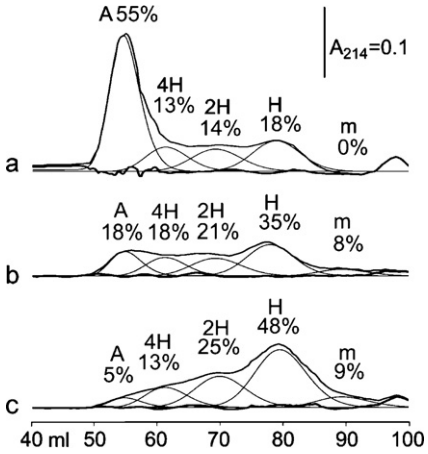

Fig. 3. Gel filtration of three CRP_{cys}-XL preparations. (a) A very active CRP_{cys}-XL preparation typically used for platelet aggregation studies, effective at <15 ng mL^{-1}. (b and c) Less active preparations, requiring 30 ng mL^{-1} (b) or 120 ng mL^{-1} (c) for a similar effect (see Suppl. Fig. S1).
m: monomer – Stokes' Radius (R) = 1.3 nm; H: 1 triple helix, R = 2.3 nm; 2H: 2 triple helices, R = 3.5 nm; 4H: ∼3–5 triple helices, R = 5.1 nm; A: aggregate (up to 80 triple helices), R = 8.6 nm.

2.6. Mass spectrometry of products

Peptide samples were desalted by adsorbing to a preconditioned μC18 Ziptip (Millipore). For electrospray, they were eluted with 70% MeOH/0.2% formic acid, and delivered to the mass spectrometer by direct infusion at 4 μL min^{-1} using 70% MeOH/0.2% formic acid as mobile phase, with a capillary temperature of 80 °C. Internal calibration data was also collected using either ubiquitin or myoglobin. For MALDI (Waters MicroMX), they were washed with 0.1% trifluoroacetic acid and eluted with matrix solution, mixed with ferulic acid matrix (10 mg mL^{-1} in 50% acetonitrile, 0.1% trifluoroacetic acid), dried and washed with 0.1% trifluoroacetic acid. To confirm the redox state of peptide samples and a TCEP-reduced negative control, peptides were alkylated using 120 mM iodoacetamide (Sigma I6125), pH 8, for 30 min at room temperature before analysis [31].

2.7. Whole blood perfusion experiments

Blood from healthy volunteers was collected into 40 μM D-phe-pro-arg-chloromethylketone (PPACK, Cambridge Bioscience, UK), and supplemented hourly with 10 μM PPACK. It was incubated with 1 μM 3,3′-dihexyloxacarbocyanine iodide (DIOC6, Sigma–Aldrich, UK) for 15 min before use. Acid-cleaned coverslips (Menzel-Glazer, Germany) were washed in a solution of 1 M HCl in 50% ethanol, followed by two washes with 300 mM NaCl and a final wash with water. Base-treated coverslips were washed finally with 1 M NaOH. These coverslips were incubated with a mixture of two peptides (100 μg mL^{-1} each) in a humidity chamber overnight. The peptide mixture was either CRP_{cys} and $GFOGER_{cys}$ or the cysteine-lacking CRP and GFOGER (Table 1). After removal of excess fluid, coverslips were blocked with 1% BSA in HEPES buffer (36 mM NaCl, 2.7 mM KCl, 5 mM HEPES, 10 mM glucose, 2 mM $MgCl_2$, 2 mM $CaCl_2$, pH 7.4) for 15 min. Individual coverslips were loaded into a 125 μm deep flow chamber mounted on an FV300 laser-scanning confocal microscope (Olympus, UK) and washed for 1 min with HEPES buffer. Blood was drawn through the chamber using a syringe pump for 5 min at a shear rate of 1000 s^{-1} [22]. Following each experiment, the chamber was flushed using HEPES buffer before image acquisition.

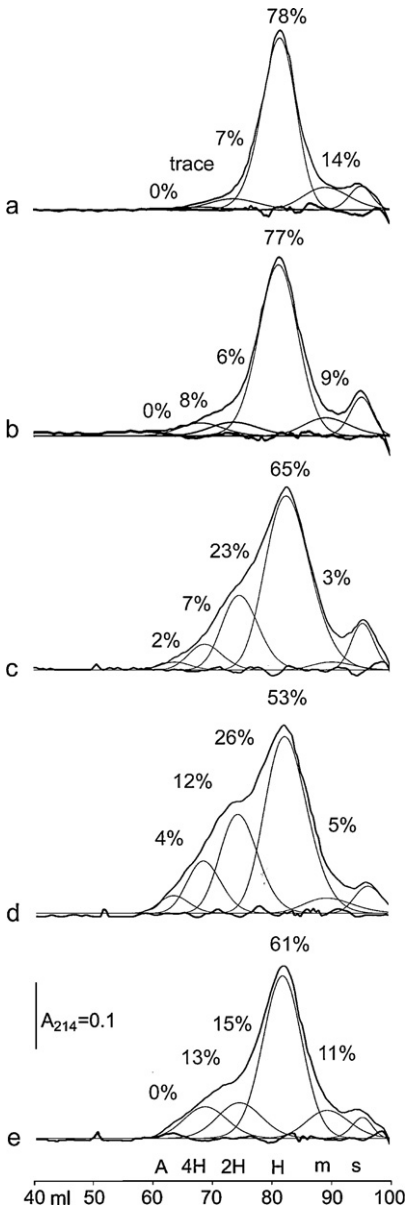

Fig. 4. Gel filtration of CRP_{cys}: (a) freshly dissolved; (b) 14d, 4 °C; (c) 9 month, 4 °C; (d) 53 month, 4 °C; (e) freeze–thawed 10× during 14 d, −20 °C. Peptide percentages are given for:
m: monomer – Stokes' Radius (R) = 1.0 nm; H: 1 triple helix, R = 1.8 nm; 2H: 2 triple helices, R = 2.9 nm; 4H: ~3–5 triple helices, R = 3.5 nm; A: small aggregate, R = 4.5 nm; s: solvent (right-most peak).

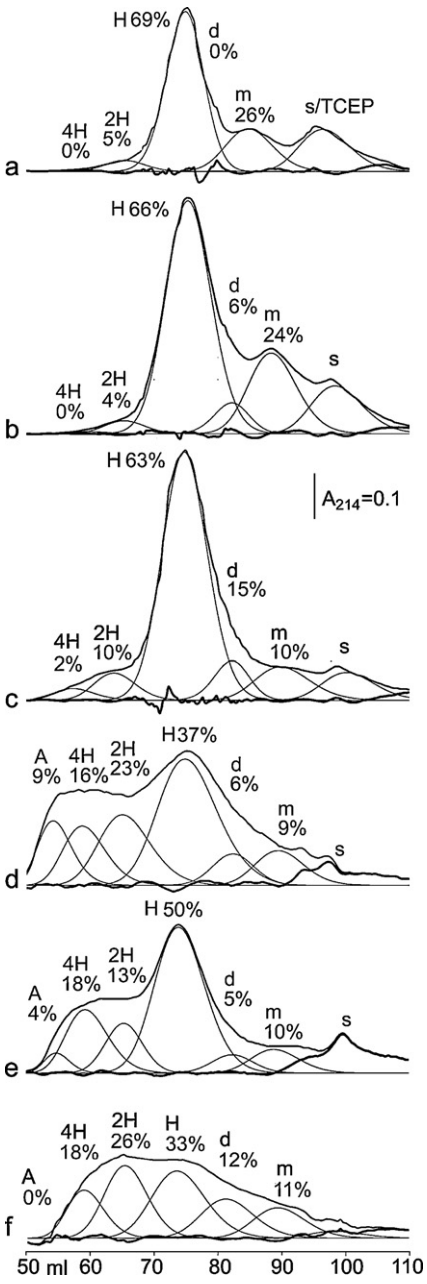

Fig. 5. Gel filtration of III-24. (a) Sample TCEP-reduced after 18 h at 4 °C; (b) 2 h at 4 °C; (c) 14 d at 4 °C (14 d at −20 °C is similar). (d) After freeze thawing 10× during a 14 d period at −20 °C; (e) 80 d at −20 °C; (f) 37 month at 4 °C.
m: monomer – Stokes' Radius (R) = 1.3 nm; H: 1 triple helix, R = 1.9 nm; 2H: 2 triple helices, R = 2.7 nm; 4H: ~3–5 triple helices, R = 4.0 nm; A: small aggregate R = 5.7 nm; s: solvent (right-most peak).

2.8. Adhesion assays

Platelet adhesion was measured by detecting phosphatase released by lyzing adherent platelets [20]. Peptide solutions (100 μL; 10 μg mL^{-1} in 0.01 M acetic acid) were added to 96-well plates and left overnight at 4 °C. Excess ligand was discarded and wells were blocked with 175 μL 5% bovine serum albumin (BSA) in calcium-free Tyrodes' buffer (CFT) for 1 h, after which the wells were washed 3 times with 175 μL 0.1% BSA in CFT. Washed mouse platelets (50 μL; 1.25×10^8 mL^{-1}) from wild-type or FcRμ-chain knockout animals which lack functional GpVI [6] were incubated in each well at room temperature for 1 h. Excess, non-bound platelets were discarded and the wells were washed 3 times. Citrate lysis buffer (150 μL: 3.53 mM p-nitrophenyl phosphate, 71.4 mM trisodium citrate, 28.6 mM citric acid, 0.1% (v/v) Triton X-100; pH 5.4) was added to each well for 1 h at room temperature. Then, 100 μL 2 M NaOH was added to each well and absorbance at 405 nm was determined using a Fluostar plate reader (BMG Labtech, Aylesbury, UK).

Coating of plates with biotinylated peptide was measured by adding peptide solutions (100 μL) to a 96-well plate for 30 min–4 h. The plate was blocked using 250 μL 5% BSA in 50 mM Tris buffer with 150 mM NaCl (TBS) and then washed with BSA-free TBS. Coated peptide was quantitated by adding 200 μL of a 1:10,000 dilution of a streptavidin–horseradish peroxidase solution (Chemicon), washing, and developing with 200 μL 3,3′,5,5′-tetramethylbenzidine substrate (Thermo Scientific). The reaction was stopped with 50 μL 2.5 M sulphuric acid, turning the solution yellow, and absorbance was measured at 450 nm.

3. Results

3.1. Gel filtration analysis of CRP_{cys}-XL

Fig. 2 shows theoretical elution profiles for macromolecules of differing Stokes Radius from a gel filtration column, see Suppl. Sections 2.10 and 2.11. These depend upon the pore sizes (a) within the column, and the axial dispersion (b) due to both inhomogeneity of flow and the solute interaction with the column (see Section 2). Using this model to deconvolute the gel filtration data, solvent effects (s), TCEP (s), peptide monomers (m) and triple helices (H) were easily fitted (Figs. 3–5). However, larger molecules seen on the elution profiles may be triple helices attached end-to-end rather than side-by-side; triple helices with attached non-helical single chains; or may simply be so large as to exceed the resolution of the method. Therefore, we defined three higher mass states as consistently as possible across the data, approximating 2 triple helices (2H), 3–5 triple helices (4H), and an aggregate of 6+ triple helices (A). A final fitted peak was the approximate mass of a peptide dimer (d), observed only in Toolkit peptide studies. This "dimer" peak may include some peptide helix that unwound during the column run, resulting in peptide monomer that elutes between helical and monomeric masses.

Fig. 3a–c shows the elution profile of three CRP_{cys}-XL preparations, following cross-linking by SPDP. This procedure may vary, occasionally yielding CRP_{cys}-XL of low potency. The preparations selected for this study were of high (3a), acceptable (3b) and low (3c) platelet-reactivity, the latter being unsuitable for use. The contribution of each molecular species and its corresponding Stokes Radius were calculated. Up to 55% of the total peptide formed soluble helix aggregates (Fig. 3a). The amount of soluble helical aggregate increased with potency in CRP_{cys}-XL-induced platelet aggregation (Suppl. Fig. 1).

3.2. Oxidation of CRP_{cys} and GPP_{cys} during storage

As would be expected from a peptide that can bind, and therefore cluster, at most three GpVI molecules [30], monomeric CRP_{cys} acts as a weak partial agonist [1] and can therefore antagonize the effect of CRP_{cys}-XL, a potent agonist at platelet GpVI. We therefore investigated the triple-helical and polymeric states of our peptides over time to see what degree of polymerization of CRP_{cys} in solution may be caused by oxidative disulfide formation.

When CRP_{cys} was freshly dissolved in cold buffer from freeze-dried stock, gel filtration showed that 78% of the peptide was triple-helical, with 14% being monomeric and ~8% being in polymers of 2–4 triple helices (Fig. 4a). Over 14 d at 4 °C, re-folding reduced the monomer content to 9%, while oxidation increased polymers of triple-helices to 14% (Fig. 4b). Freezing the solution immediately after dissolving the peptide kept it mostly reduced: peptide monomer was 11% and helical polymers 16% after 80 d (data not shown). However, when the peptide was stored for long periods at 4 °C or was repeatedly freeze–thawed, much more extensive oxidation occurred, shown in Fig. 4c–e. These polymers, however, still have smaller Stokes Radius compared to CRP_{cys}-XL due to the different cross-linking mechanism. Repeating this experiment with peptide GPP_{cys} in N_2-saturated solution resulted in negligible oxidation over 14 d. Likewise, investigating short (1–14 d) and long-term (18 month) storage of GPP_{cys} in air-saturated buffer gave very similar results to those obtained for CRP_{cys} (data not shown).

3.3. Oxidation of Toolkit peptide III-24 during storage

We used a TCEP-reduced sample of III-24 to establish the elution time of its triple-helix (Fig. 5a). The non-reduced control (Fig. 5b) showed an additional feature, a minor peak corresponding to a disulfide-linked peptide dimer (labeled d). Non-reduced solutions equilibrated at 4 °C for 12 h or longer (Fig. 5c) contained significantly less monomeric peptide (labeled m) than the TCEP-reduced sample. As peptide was flash-frozen from a room temperature solution before freeze-drying for storage, the re-dissolved peptide in Fig. 5b reflects the initial room-temperature equilibrium composition, with more monomer. Monomer content falls over 14 d at 4 °C (Fig. 5c), partly due to peptide oxidation and increased dimer content, but mainly due to folding as triple helices (as in Fig. 4a and b), resulting in more 2- and 4-helix polymers (12% in total).

More oxidation was caused by freeze–thawing 10 times over 14 d at −20 °C (Fig. 5d), or leaving the peptide at −20 °C over 80 d (Fig. 5e), or leaving the peptide at 4 °C for 37 months (Fig. 5f). Storing peptide III_24 in N_2-saturated solution with repeated freeze–thawing over 14 d slowed oxidation four-fold (data not shown).

Long-term storage of other Toolkit peptides resulted in variable polymerization. Just 12% of 37 month-old III-04 had formed helical polymers while 44% of 41-month old II-56 was polymeric, similar to the level shown for III-24 in Fig. 5f.

3.4. Oxidative cross-linking stabilizes the helix

A sample of III-24 (T_m 51 °C at 2.5 mg mL^{-1}) stored for 48 months at 4 °C was 47% triple-helical when analyzed by gel filtration at 40 °C. However, after 10 min reduction with 2 mM TCEP, the proportion of triple-helical peptide was 18%. Helicity was ~75% if gel filtration was run at 10 °C, regardless of the presence of TCEP.

3.5. Component analysis of oxidized peptide mixtures

Peptides were heat-denatured after storage at 4 °C for 9 months or longer. They were analyzed by gel filtration at 60 °C, and by MALDI and electrospray mass spectrometry immediately after heating to 60 °C. Their cysteine thiol content was determined using Ellman's reagent. This allowed us to characterize the peptide polymer mixture (Suppl. Figs. S2–S5, Tables S1 and S2, Sections 3.8, 4.4, 4.5). Briefly, >90% of cysteine in peptides aged for 9 months or more is oxidized, and cross-linked such that 5–13% of the peptide is monomeric (mostly cyclic), 7–50% is dimeric, correlating with peptide stability and purity, where CRP_{cys} has less dimer than the other peptides, and the remainder is polymeric. Positive controls using fresh peptide were ~95% reduced as expected.

3.6. Dynamic light scattering (DLS) of a Toolkit peptide

Gel filtration revealed that, in the presence of 2 mM TCEP, peptide III-24 at 2.5 mg mL^{-1} was almost free of any component bigger than a single helix, no matter what temperature (4–50 °C) was maintained before loading onto the column (see, for example, Fig. 5a). To confirm this, we undertook DLS experiments under reducing conditions in neutral buffer. There was no evidence of any species larger than around 16.5 kDa, equivalent to a single helix. We could not resolve peptide monomer from helix, so mass and Stokes Radius shown in Table 2 represent average values, decreasing with increasing temperature due to helix denaturation. Stokes Radius correlated well with values obtained from gel filtration, and are as expected for rod-like molecules of this mass.

3.7. Adhesion assays using cysteine- and non-cysteine-containing peptides

We evaluated the coating of biotinylated peptides with or without cysteine to 96-well plates, detected as described in Section 2. We could detect coating of the plastic by cysteine-containing

Table 2
DLS data for peptide III-24 treated with 10 mM TCEP. At 50 °C, DLS is not stable, and the % intensity data is not reliable. The Stokes Radius "*R*" is used to calculate the molecular weight.

T (°C)	*R* (nm)	MW (kDa)	Intensity (%)
4	2.7	12	90
10	3.2	16	95
20	2.9	14	92
30	2.5	11	88
40	2.1	8	76
50	1.1	3	n/a

biotinylated peptide (B-GFOGER$_{cys}$), but biotinylated peptides lacking cysteine-adhered poorly (B-GFOGER) or not at all (B-CRP) (Fig. 6a). Additionally, all peptides containing motifs that bind integrin α2β1 or GpVI and terminal cysteine supported platelet adhesion (CRP$_{cys}$, GFOGER$_{cys}$, B-GFOGER$_{cys}$, Fig. 6b). The negative control, GPP$_{cys}$, showed that (GPO)$_n$ and not (GPP)$_n$ was required for mouse platelet adhesion, as anticipated [11]. Likewise, no platelet adhesion was detected using other negative control peptides, containing GpVI- or integrin-binding sequences but not terminal cysteine. Lastly, comparison of platelets from wild-type and FcRγ$^{-/-}$ knockout mice, which lack GpVI [6], confirm that platelet adhesion to CRP is mediated by GpVI interacting with (GPO)$_n$ and not via some unsuspected interaction with terminal cysteine residues. This forces us to conclude that cysteine is required for tethering the peptide to the plate.

Finally, using whole blood perfusion experiments [22], we observed thrombus formation upon GFOGER$_{cys}$ and CRP$_{cys}$-prepared surfaces, but not upon GFOGER and CRP-prepared surfaces (Fig. 7), where the latter peptides lack cysteine. This was the case regardless of whether the slide had been pre-washed with acid or alkali, although washing the surface with sodium hydroxide prior to coating led to the deposition of noticeably larger thrombi.

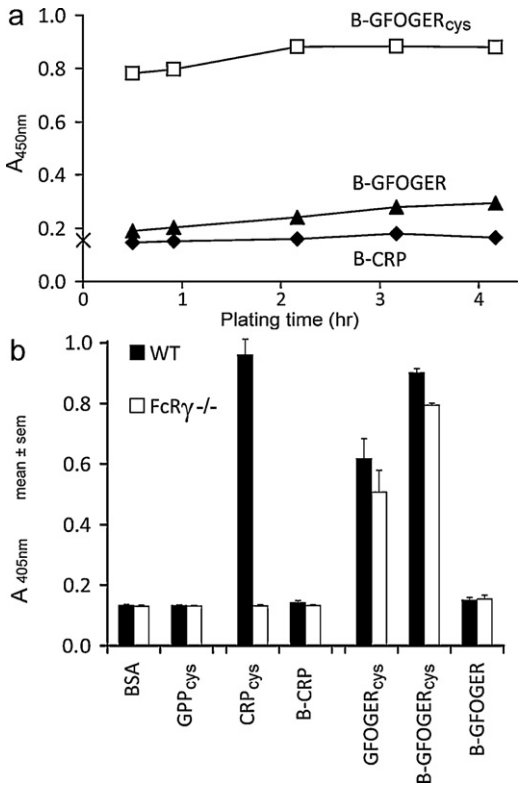

Fig. 6. Adhesion experiments. (a) Streptavidin binding to coated peptide. Data for 1:10,000 streptavidin dilution is shown: similar results were obtained at 1:3000 and 1:1000 dilutions. (b) Wild type and FcR-gamma knockout mice platelet adhesion to immulon-2B 96-well plates treated with various biotinylated and non-biotinylated peptides.

4. Discussion

4.1. Advantages of cysteine-containing peptides

Inclusion of cysteine in collagenous peptides offers the possibility of cross-linking, an important property exemplified by CRP$_{cys}$-XL, a potent platelet agonist, whereas monomeric CRP is an antagonist or at best a partial agonist [18]. Polymerization of the peptide by deliberate, random cross-linking using SPDP introduces higher-order structure into the peptide, which can only then support the clustering of GpVI which leads to activatory signaling in platelets. This parallels the behavior of collagen itself, where fibrillar but not monomeric collagen preparations can activate platelets. The active peptide aggregate within CRP$_{cys}$-XL can be calculated to have an average Stokes Radius of 8.6 nm from its elution volume (Fig. 3). This is similar to the 8.9 nm Stokes Radius of the rod-like 86 kDa glycoprotein, extensin [32], which has the mass and length of ~8 CRP$_{cys}$ triple helices. Therefore, the active CRP$_{cys}$-XL aggregate must contain at least 8, and probably many more, CRP$_{cys}$ triple helices, as the peptide helices are unlikely to align lengthwise [8]. The elution volume from gel filtration of CRP$_{cys}$ also showed that a single CRP$_{cys}$ helix at 10 °C has a Stokes' Radius of ~2 nm (its length being 11 nm). As the molecular mass varies with the cube of the Stokes Radius, we can estimate that a CRP$_{cys}$-XL aggregate contains up to 80 CRP$_{cys}$ triple helices.

A second valuable property of terminal cysteine residues in peptides is that they enhanced the adhesion of the peptide to plastics (Fig. 6a), glass (Fig. 7), and gold [26] without further modification. This may be a specific property of cysteine sidechains, or may result from multiple, co-operative, weak interactions that become possible with oxidized polymeric peptides. Using peptides lacking cysteine may mean that binding sites remain undiscovered as both peptide and target protein may be washed off surfaces. It is also likely that less peptide will be needed for surface coating. Of note, while B-GFOGER adhered to plastic poorly compared to B-GFOGER$_{cys}$, it adhered better than B-CRP (Fig. 6a). We speculate that the GFOGER sidechains may improve the limited peptide adhesion.

Third, light-scattering experiments under reducing conditions confirmed that III-24 denatures to single chains at temperatures of 50 °C or higher (Table 2), and gel filtration showed that cross-linking resulting from chance oxidation can stabilize the triple helices. Stabilization alternatively could be achieved either by replacing the (GPP)$_5$ host sequence on either side of the guest sequence with a more stable (GPO)$_5$ host sequence, or by lengthening the peptide. However, the former means that every peptide could be recognized by GpVI, LAIR, and possibly other proteins [23], complicating analysis, while the latter not only increases the difficulty and expense of the synthesis, but is likely to reduce the solubility of the peptide.

Fourth, we have been able to separate various sizes of triple-helical cross-linked fractions from a gel filtration column, and it would be possible to assay them individually for binding activity. Because they are stable enough to remain in one state for the duration of a column run at 10 °C, they will at least be useful for experiments under cold conditions. Previous work has suggested that the half-life of any one folded helix is at least a few hours provided it is more than 20 °C below its melting temperature [27].

Finally, we have shown that most of the peptide monomer present in a sample becomes oxidized when stored for a long time at 4 °C (Suppl. Sections 3.8–3.11), and therefore cyclic. Gel filtration can be used to isolate cyclic peptide as a potentially useful control material which cannot form triple helices.

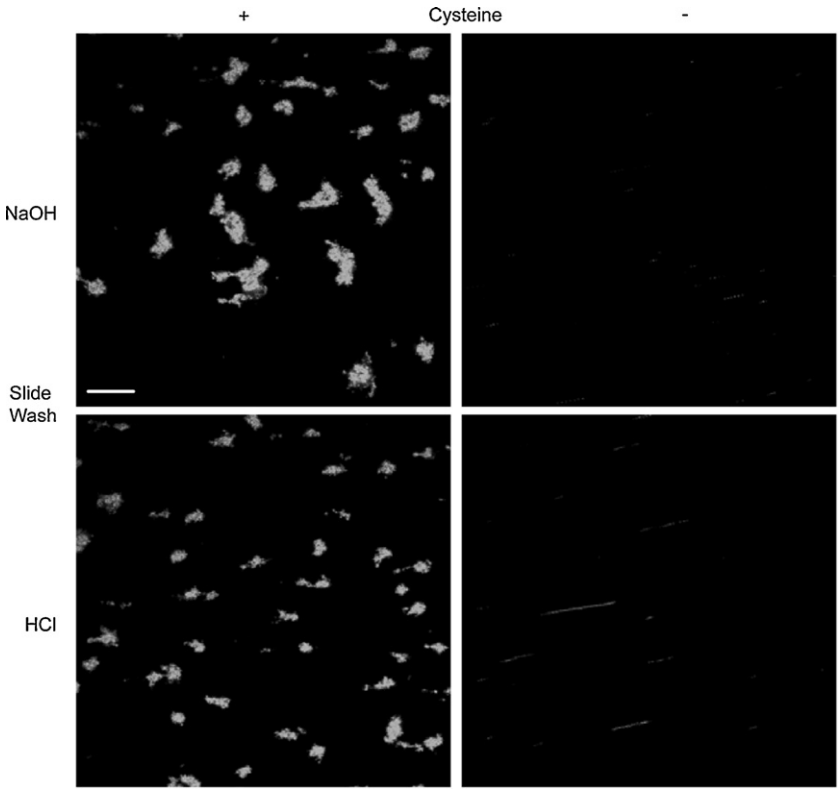

Fig. 7. Confocal microscopy of blood-perfused surfaces. Glass slides were washed with HCl or NaOH before coating with a mixture of CRP_{cys} and $GFOGER_{cys}$ or CRP and GFOGER (see Section 2). Peptides without cysteine did not support platelet binding or thrombus formation (scale bar = 50 μM).

4.2. Oxidation of peptides during storage and handling

Multiple freeze–thawing while storing at −20 °C resulted in considerably faster oxidation over the same period of both III-24 and CRP_{cys} compared to simply storing the peptide at 4 °C (Figs. 4e and 5d). This effect meant that peptide frozen for as much as 80 d and then thawed could have an oxidation profile similar to a sample stored for much longer at 4 °C (Fig. 5).

Storage over longer periods at 4 °C (9+ months), with occasional use, caused all peptides to oxidize almost to completion (Suppl. Section 3.10). After denaturation of peptide triple helices, analysis of these peptides showed that CRP_{cys} had formed larger peptide polymers than GPP_{cys} (Suppl. Section 3.9), and this was reflected in it forming larger aggregates. While this may be because the CRP_{cys} forms more stable triple helices, the data from Toolkit peptides suggested otherwise, where lower stability III-24 had formed both larger peptide polymers than III-04 over time (Tables S1 and S2), and these also resulted in larger helical aggregates than peptide III-04.

4.3. Disadvantages of cysteine-containing peptides

Oxidation of cysteine has been shown to be unavoidable under normal storage conditions (Figs. 3–5). This can be confirmed arithmetically. At a stock concentration of 1 mg mL^{-1}, the molarity of these peptides is typically 0.2–0.7 mM. The oxygen content of air-saturated water is 0.41 mM at 4 °C, reducing to 0.26 mM at 25 °C. A single oxygen molecule can oxidize four cysteines to two cysteine cross-links, so there is at least a two-fold excess of oxygen over cysteine. Even if one retains stocks at 5 mg mL^{-1} to reduce this effect, the 500 μL of air that is a typical headspace within an Eppendorf tube contains 4.4 μmol of oxygen at atmospheric pressure. Over time, this can saturate a 5 mg mL^{-1} peptide solution kept at 4 °C, providing enough oxygen for complete peptide oxidation. So, unless peptide solutions are stored under nitrogen, or flash-frozen from a nitrogen-saturated state, cysteine thiols will slowly oxidize until they reach redox equilibrium. This will be especially so during freeze–thawing in air, where raising the temperature to room temperature and back to freezing causes the movement of oxygen into and out of solution due to its differential solubility at these temperatures, and, in addition, causes peptide concentration to increase locally during freezing.

Second, until oxidation is complete after protracted storage, there is no simple correlation between age and peptide oxidation state, as cross-linking appears to be dependent on both peptide identity and handling (Figs. 3–5, and Suppl. Sections 3.8–3.11, 4.4–4.5).

Third, the presence of terminal cysteines makes it more likely that the peptide will precipitate upon extended storage at high concentrations, as a consequence of disulfide-mediated formation. Visible precipitation has not occurred within 1 mg mL^{-1} solutions of Toolkit peptides stored long-term in 10 mM acetic acid at 4 °C, but we have observed precipitation of 5 mg mL^{-1} solutions of Toolkit peptides at neutral pH even under reduced conditions (data not shown). Another collagen peptide lacking cysteine has been shown to form higher-order structures at concentrations as low as 1.4 mg mL^{-1} due to interactions involving aromatic residues [9], so aggregation will be a co-operative effect involving cross-linking and non-covalent interactions. Heating precipitated peptide helix aggregates usually re-dissolves them as monomers and small peptide polymers, and they can be cooled to allow refolding, regenerating at least a temporary working solution at high concentration. Precipitation in the form of fibril formation may of course be desirable if a peptide is designed to form fibrils [13,21], which may have other experimental applications.

Formation of soluble micro-aggregates of peptide triple helices by air-induced oxidative or SPDP-induced chemical cross-linking can be reversed by adding TCEP to the solution if the subsequent

usage is compatible with its presence or easy removal. Likewise, air-induced oxidation can be minimized by storage under nitrogen; by dissolving fresh peptide from a freeze-dried stock; or by aliquotting and storing at −80 °C, although oxidation will still occur during the freeze–thawing process, and slowly while frozen (compare Fig. 5c and d – oxidation rates at −80 °C were not tested). Finally, a non-cysteine containing peptide could be synthesized if no other method is acceptable. We have not observed any oxidation of peptide while it is stored in a freeze-dried state at −20 °C.

5. Conclusion

We have characterized size profiles of cysteine-containing collagen peptides after either chemical cross-linking (CRP_{cys}-XL), where such cross-linking allows formation of soluble aggregates (Stokes Radius 8.6 nm) capable of activating platelets, or after air-induced cysteine oxidation upon storage. The latter gives rise to smaller polymers (1–6 triple helices) resulting from inter- and intra-helix oxidation of cysteine to disulphide bonds. This air-induced oxidation can be slowed by careful storage and handling.

We have also shown that cysteine facilitates strong adhesion of small collagen peptides to plastic and to glass, a valuable aid for surface-dependent analyses such as solid-phase adhesion assays.

Supporting information

(a) Methods for gel filtration analysis are in Suppl. Sections 2.9–2.13. (b) Aggregation of platelets by CRP_{cys}-XL is shown in Fig. S1. (c) Peptide oxidation states are shown in Figs. S2–S5 and Tables S1 and S2. Results are described in Suppl. Sections 3.8–3.11 and discussed in Sections 4.4 and 4.5.

Acknowledgement

This work was supported by the British Heart Foundation (PG/08/011/24416).

Appendix A. Supplementary data

Supplementary data associated with this article can be found, in the online version, at http://dx.doi.org/10.1016/j.peptides.2012.04.013.

References

[1] Asselin J, Knight CG, Farndale RW, Barnes MJ, Watson SP. Monomeric (glycine-proline-hydroxyproline)10 repeat sequence is a partial agonist of the platelet collagen receptor glycoprotein VI. Biochem J 1999;339(Pt 2):413–8.
[2] Ellman GL. A colorimetric method for determining low concentrations of mercaptans. Arch Biochem Biophys 1958;74:443–50.
[3] Farndale RW, Lisman T, Bihan D, Hamaia S, Smerling CS, Pugh N, et al. Cell–collagen interactions: the use of peptide Toolkits to investigate collagen–receptor interactions. Biochem Soc Trans 2008;36:241–50.
[4] Fratzl P. Collagen structure and mechanics. Springer; 2008.
[5] Gauba V, Hartgerink JD. Surprisingly high stability of collagen ABC heterotrimer: evaluation of side chain charge pairs. J Am Chem Soc 2007;129:15034–41.
[6] Jarvis GE, Raynal N, Langford JP, Onley DJ, Andrews A, Smethurst PA, et al. Identification of a major GpVI-binding locus in human type III collagen. Blood 2008;111:4986–96.
[7] Kadler K. General overview of collagens. Academic Press; 1995.
[8] Kar K, Amin P, Bryan MA, Persikov AV, Mohs A, Wang YH, et al. Self-association of collagen triple helic peptides into higher order structures. J Biol Chem 2006;281:33283–90.
[9] Kar K, Ibrar S, Nanda V, Getz TM, Kunapuli SP, Brodsky B. Aromatic interactions promote self-association of collagen triple-helical peptides to higher-order structures. Biochemistry 2009;48:7959–68.
[10] Kehrel B, Wierwille S, Clemetson KJ, Anders O, Steiner M, Knight CG, et al. Glycoprotein VI is a major collagen receptor for platelet activation: it recognizes the platelet-activating quaternary structure of collagen, whereas CD36, glycoprotein IIb/IIIa, and von Willebrand factor do not. Blood 1998;91:491–9.
[11] Knight CG, Morton LF, Onley DJ, Peachey AR, Ichinohe T, Okuma M, et al. Collagen–platelet interaction: Gly-Pro-Hyp is uniquely specific for platelet Gp VI and mediates platelet activation by collagen. Cardiovasc Res 1999;41:450–7.
[12] Knight CG, Morton LF, Peachey AR, Tuckwell DS, Farndale RW, Barnes MJ. The collagen-binding A-domains of integrins alpha(1)beta(1) and alpha(2)beta(1) recognize the same specific amino acid sequence, GFOGER, in native (triple-helical) collagens. J Biol Chem 2000;275:35–40.
[13] Krishna OD, Jha AK, Jia X, Kiick KL. Integrin-mediated adhesion and proliferation of human MSCs elicited by a hydroxyproline-lacking, collagen-like peptide. Biomaterials 2011;32:6412–24.
[14] Lebbink RJ, Raynal N, de Ruiter T, Bihan DG, Farndale RW, Meyaard L. Identification of multiple potent binding sites for human leukocyte associated Ig-like receptor LAIR on collagens II and III. Matrix Biol 2009;28:202–10.
[15] Leo JC, Elovaara H, Bihan D, Pugh N, Kilpinen SK, Raynal N, et al. First analysis of a bacterial collagen-binding protein with collagen Toolkits: promiscuous binding of YadA to collagens may explain how YadA interferes with host processes. Infect Immun 2010;78:3226–36.
[16] Lisman T, Raynal N, Groeneveld D, Maddox B, Peachey AR, Huizinga EG, et al. A single high-affinity binding site for von Willebrand factor in collagen III, identified using synthetic triple-helical peptides. Blood 2006;108:3753–6.
[17] Mohs A, Silva T, Yoshida T, Amin R, Lukomski S, Inouye M, et al. Mechanism of stabilization of a bacterial collagen triple helix in the absence of hydroxyproline. J Biol Chem 2007;282:29757–65.
[18] Morton LF, Hargreaves PG, Farndale RW, Young RD, Barnes MJ. Integrin alpha 2 beta 1-independent activation of platelets by simple collagen-like peptides: collagen tertiary (triple-helical) and quaternary (polymeric) structures are sufficient alone for alpha 2 beta 1-independent platelet reactivity. Biochem J 1995;306(Pt 2):337–44.
[19] Olsen BR, Ninomiya YC. In: Krees T, Vale R, editors. Extracellular matrix, anchor, and adhesion proteins. Oxford: Oxford University Press; 1998. p. 380–408.
[20] Onley DJ, Knight CG, Tuckwell DS, Barnes MJ, Farndale RW. Micromolar Ca^{2+} concentrations are essential for Mg^{2+}-dependent binding of collagen by the integrin alpha 2beta 1 in human platelets. J Biol Chem 2000;275:24560–4.
[21] Przybyla DE, Chmielewski J. Higher-order assembly of collagen peptides into nano- and microscale materials. Biochemistry 2010;49:4411–9.
[22] Pugh N, Simpson AM, Smethurst PA, de Groot PG, Raynal N, Farndale RW. Synergism between platelet collagen receptors defined using receptor-specific collagen-mimetic peptide substrata in flowing blood. Blood 2010;115:5069–79.
[23] Raynal N, Hamaia SW, Siljander PR, Maddox B, Peachey AR, Fernandez R, et al. Use of synthetic peptides to locate novel integrin alpha2beta1-binding motifs in human collagen III. J Biol Chem 2006;281:3821–31.
[24] Reyes CD, Garcia AJ. Engineering integrin-specific surfaces with a triple-helical collagen-mimetic peptide. J Biomed Mater Res A 2003;65:511–23.
[25] Russell LE, Fallas JA, Hartgerink JD. Selective assembly of a high stability AAB collagen heterotrimer. J Am Chem Soc 2010;132:3242–3.
[26] Sasaki YC, Yasuda K, Suzuki Y, Ishibashi T, Satoh I, Fujiki Y, et al. Two-dimensional arrangement of a functional protein by cysteine–gold interaction: enzyme activity and characterization of a protein monolayer on a gold substrate. Biophys J 1997;72:1842–8.
[27] Slatter DA, Miles CA, Bailey AJ. Asymmetry in the triple helix of collagen-like heterotrimers confirms that external bonds stabilize collagen structure. J Mol Biol 2003;329:175–83.
[28] Slatter DA, Foley LA, Peachey AR, Nietlispach D, Farndale RW. Rapid synthesis of a register-specific heterotrimeric type I collagen helix encompassing the integrin alpha2beta1 binding site. J Mol Biol 2006;359:289–98.
[29] Smethurst PA, Joutsi-Korhonen L, O'Connor MN, Wilson E, Jennings NS, Garner SF, et al. Identification of the primary collagen binding surface on human glycoprotein VI by site-directed mutagenesis and by a blocking phage antibody. Blood 2004;103:903–11.
[30] Smethurst PA, Onley DJ, Jarvis GE, O'Connor MN, Knight CG, Herr AB, et al. Structural basis for the platelet–collagen interaction: the smallest motif within collagen that recognizes and activates platelet glycoprotein VI contains two glycine-proline-hydroxyproline triplets. J Biol Chem 2007;282:1296–304.
[31] Smythe CV. The reaction of iodoacetate and of iodoacetamide with various sulfhydryl groups, with urease, and with yeast preparations. J Biol Chem 1936;114:601–12.
[32] Stafstrom JP, Staehelin LA. The role of carbohydrate in maintaining extensin in an extended conformation. Plant Physiol 1986;81:242–6.
[33] Xu H, Raynal N, Stathopoulos S, Myllyharju J, Farndale RW, Leitinger B. Collagen binding specificity of the discoidin domain receptors: Binding sites on collagens II and III and molecular determinants for collagen IV recognition by DDR1. Matrix Biol 2011;30:16–26.